Asian Journal of Chemistry; Vol. 38, No. 1 (2026), 180-186
ASIAN JOURNAL OF CHEMISTRY
https://doi.org/10.14233/ajchem.2026.34993

Sulfonated Graphene Oxide Catalyzed Transformation of Pyrazole-Oxazolidine Derivatives and their Antimicrobial Activities

V. MURALI KRISHNA MADASU[1], MANURI BRAHMAYYA[2,*], S. DEEPTHI[2], A. HARINATH[3], LAKSHMI REKHA BUDDIGA[4], J. CHANDRA SEKHARA RAO[5], M. PADMA[1,*], PRAVEEN CHOPPARA[6], D. SAMSONU[7] and A. VENKATESWARA RAO[8]

[1]Deparment of Engineering Chemistry, AU College of Engineering, Andhra University, Visakhaptnam-530003, India
[2]MLR Institute of Technology, Laxman Reddy Avenue, Dundigal Police Station Road, Hyderabad-500043, India
[3]Department of Chemistry, C.M. Science College, Lalit Narayan Mithila University, Dharbanga-846004, India
[4]Department of Humanities & Science, CMR Technical Campus ((Autonomous Engineering College), Medchal, Hyderabad-501401, India
[5]Department of Physics, Government Degree College, Rajam-532127, India
[6]Department of Chemistry, Pithapur Rajah's Government College (A), Kakinada-533001, India
[7]School of Chemistry, Andhra University, Visakhapatnam-530003, India
[8]Advanced Functional Materials Research Centre, Department of Physics, Koneru Lakshmaiah Education Foundation, Guntur-522502, India

*Corresponding authors: E-mail: manuribrahmayya@mlrit.ac.in; mpadma.aueng@gmail.com

Received: 1 October 2025 *Accepted*: 22 November 2025 *Published online*: 31 December 2025 AJC-22236

In this work, biologically active novel (*E*)-5-((1-phenyl-3-(4-R-phenyl)-1*H*-pyrazol-4-yl)methylene)-3-(4-chlorophenyl)oxazolidine-2,4-dione derivatives are synthesized and characterized. Initially, 5-azanyl(4-chlorophenyl)carbamate (**3**) was obtained from 4-chloroaniline (**1**) *via* carbonation with CO_2 (**2**) in liquid ammonia, followed by O-carboxymethylation with sodium 2-chloroacetate to afford sodium 2-(((4-chlorophenyl)carbamoyl)oxy)acetate (**4**). Subsequently, compound **4** was cyclized to yield 3-(4-chlorophenyl)oxazolidine-2,4-dione (**5**) using sulfonated graphene oxide (SGO) as metal free nanocatalyst. Later, benzohydrazide (**6**) was condensed with various types of carboxylic acids (**7**) in presence of glacial acetic acid to obtain (*E*)-(4-*R*-phenyl)ethylidene hydrazone (**8**). It is further treated with $POCl_3$ at 80 ºC for 4 h to obtain substituted pyrazole derivatives (**9a-h**). Finally, substituted pyrazole derivatives (**9a-h**) treated with sulfonated graphene oxide (SGO) catalyzed product 3-(4-chlorophenyl)oxazolidine-2,4-dione (**5**) to obtain targeted heterocyclic molecules **10a-h**. This protocol demonstrates significant advantages in efficiency, ecological sustainability and catalyst reusability. Furthermore, the synthesized 1,3-oxazolidine-2,4-dione derivatives were evaluated for their antibacterial properties. The findings highlight the catalytic potential of SGO in the synthesis of 1,3-oxazolidine-2,4-dione derivatives as well as in broader applications in green organic transformations.

Keywords: Hydrazine, Nano catalysis, Carbon dioxide, Cyclization, Heterocycles, Antibacterial activities.

INTRODUCTION

Pyrazole derivatives are commonly synthesized through conventional heterocyclic reaction methods, yet these approaches often suffer from significant limitations, including prolonged reaction times, the need for harsh or strongly acidic conditions and generally modest product yields [1]. The use of different catalysts and solvents, such as anchored sulfonic acid on silica-layered $NiFe_2O_4$ [2], ceric ammonium nitrate [3], chitosan nanoparticles [4], $Yb(OTf)_3$ [5], bismuth nitrate [6], La_2O_3 [7], sodium perchlorate [8] and PtNPs@GO [9], has been developed in recent years in an effort to improve reaction conditions and product yield. Although many of these catalysts offer notable advantages, they also present several drawbacks such as reliance on costly materials, long reaction times, basic organic reagents and solvents, low yields, limited generality and environmental concerns arising from chemical exposure, which make them less suitable for green chemistry applications.

In this context, sulfonated graphene oxide (SGO), an efficient solid heterogeneous acid catalyst, is emerging as key catalyst because to its high density of sulfonic acid groups and large surface area provide abundant, easily accessible active sites for efficient catalysis [10,11]. Furthermore, its improved hydrophilicity enhances dispersion and interaction with reactants, making it highly effective for diverse organic

transformations [12,13]. Considering these observations and our ongoing interest in pyrazole derivatives as potential bioactive heterocycles, we present the sulfonated reduced graphene oxide (SGO) catalyzed synthesis of novel hybrid (*E*)-5-((1-phenyl-3-(4*R*-phenyl)-1*H*-pyrazol-4-yl)methylene)-3-(4-chlorophenyl)-oxazolidine-2,4-dione derivatives. This method offers several advantages, including short reaction times, excellent yields, environmentally benign conditions, broad functional-group tolerance, and catalyst recoverability, among others.

EXPERIMENTAL

All reagents, chemicals and solvents were obtained from commercial suppliers and used as received, without further purification. The reactions were performed under an inert nitrogen atmosphere using oven-dried glassware. LC-MS analyses were carried out on an Agilent LC-MSD system coupled to an Agilent 1200 Series Binary LC instrument. ^{1}H and ^{13}C NMR spectra were recorded at 298 K on a 400 MHz Gemini Varian spectrometer, with tetramethylsilane (TMS) or residual solvent signals serving as internal references; DMSO-d_6 or analytical-grade $CDCl_3$ were used as NMR solvents. Column chromatography was performed on silica gel (300–400 mesh), and reagent-grade solvents were used for all chromatographic and extraction procedures. The prepared catalyst was characterized by X-ray diffraction (XRD). Morphological features were examined by scanning electron microscopy (SEM) coupled with EDS elemental analysis and high-resolution transmission electron microscopy (HR-TEM; Japan) was used to obtain nanoscale structural images of the catalyst.

Synthesis of sulfonated reduced graphene oxide (SGO): Sulfonated reduced graphene oxide (SGO, $GOPhSO_3H$) was prepared according to the literature reports [14,15] with minor modifications. Initially, 40 mg of GO taken in a round-bottom glass flask containing 40 mL of deionized water was mixed well at room temperate and then sonicated (ultrasonic bath, 40 kHz) the solution. Initially, 0.2 g of $NaBH_4$ was gradually added to the GO solution (pH 9-10). The resulting dispersion was heated to 80 ºC and subsequently centrifuged to obtain partially reduced graphene oxide (rGO). The rGO was then sonicated in 40 mL of distilled water in an ultrasonic bath for 15-20 min and cooled. Separately, a mixture of 40 mg sulfanilic acid, 1 mL of 1 N HCl and 5.5 mL of water was stirred at 0 ºC to generate the corresponding diazonium salt. This diazonium salt was then mixed with 14.5 mg of KNO_2 solution. The prepared diazonium solution was added dropwise to the rGO dispersion at 0 ºC, and the reaction mixture was stirred at room temperature for 10 h. The resulting black precipitate was collected by centrifugation for 15 min, washed five times with distilled water, filtered under reduced pressure and finally dried at 60 ºC for 2-3 h.

Acidic characteristics of sulfonated graphene oxide: A solution of 50 mg of SGO and 50 mL of base solution (0.01 M NaOH or 0.01 M Na_2CO_3) was prepared in a 250 mL volumetric flask and shaken for at least 2 days [16]. Bases that remained unreacted were classified as pre-reaction bases, whereas those that interacted with the acidic functionalities of SGO were termed post-reaction bases. Titration was performed using methyl red as indicator, in which 10 mL aliquots of each reaction mixture were titrated with standardized 0.01 M HCl. The acidity, expressed as the concentration of surface functional groups per gram of SGO, was calculated according to the following equation:

$$N_{SF} = \frac{C_{HCl} \times (V_{HCl,pre} - V_{HCl,post})}{M_{SGO}}$$

where N_{SF} = surface acidity (mmol g^{-1}), C_{HCl} = concentration of titrant (mol L^{-1}), V_{pre} = volume of HCl for the pre-reaction base (mL), V_{post} = volume of HCl for the post-reaction base (mL); and M_{SGO} = mass of SGO used in titration (g).

General synthesis procedure for (*E*)-5-((1-phenyl-3-(*p*-tolyl)-1*H*-pyrazol-4-yl)methylene)-3-(4-chlorophenyl)-oxazolidine-2,4-dione derivatives (10a-h): The synthesis of the pyrazole-oxazolidine derivatives is achieved in multi-steps:

Synthesis of 3-(4-chlorophenyl)oxazolidine-2,4-dione (5): In an ice bath (0-5 ºC), 4-chloroaniline (**1**, 1.0 equiv.) was dissolved in liquid NH_3 (10-15 mL/g of amine). Dry CO_2 was then bubbled through the cold solution at 1 atm. pressure for 20 min. The reaction mixture was sealed, allowed to warm to room temperature and stirred for an additional 1 h. Excess ammonia was removed by venting under a fume hood at 0 ºC. The resulting residue was triturated with cold ether to yield ammonium 4-chlorophenylcarbamate salt (**3**) as an off-white solid, Then, compound **3** (1.0 equiv.) dissolved in THF (10 mL) was added to sodium 2-chloroacetate (1.1-1.2 equiv.) while stirring the solution at room temperature for 2-3 h. The progress of the reaction was monitored by TLC (EtOAc/hexane, 4:1). Upon completion, the mixture was poured into ice-cold water, the precipitate was collected by filtration, washed with chilled water and dried under vacuum to obtain sodium 2-(((4-chlorophenyl)carbamoyl)oxy)acetate salt (**4**). Lastly, compound **4** was suspended in a round-bottom flask containing toluene (10 mL) and 10 mg of SGO nanocatalyst. The mixture was heated to 60 ºC under a nitrogen atmosphere and stirred for 1-2 h. After complete dissolution of the solid and cessation of CO_2 evolution, the reaction mixture was cooled to room temperature, diluted with ethyl acetate and the organic layer was washed with brine and dried over anhydrous $MgSO_4$. The product was purified by recrystallization from an ethyl acetate/hexane mixture to obtain 3-(4-chlorophenyl)oxazolidine-2,4-dione (**5**) (**Scheme-I**).

Catalytic activity: Sodium 2-(((4-chlorophenyl)carbamoyl)oxy)acetate (**4**) was heated to 60 ºC and catalyzed with different catalysts as well as solvent under a N_2 atmosphere for 1-2 h. Upon complete dissolution and complete CO_2 evolution, the mixture was cooled to room temperature, diluted with ethyl acetate, washed with brine, dried over Na_2SO_4 and then concentrated. The results are summarized in Table-1. Remarkably, cyclization in DMF solvent at room temperature without any catalyst produced only trace amounts of the desired product, even after 48 h.

Synthesis of substituted pyrazole derivatives (9a-h): To a stirred solution of *p*-methyl acetophenone (**7**) (1.0 equiv.) in glacial acetic acid (5-10 mL) at room temperature, added phenyl hydrazine (**6**) (1.05-1.10 equiv.) dropwise. Refluxed the solution at 118 ºC for 1-2 h and monitored the progress of the reaction by TLC (hexane/EtOAc 7:3). On

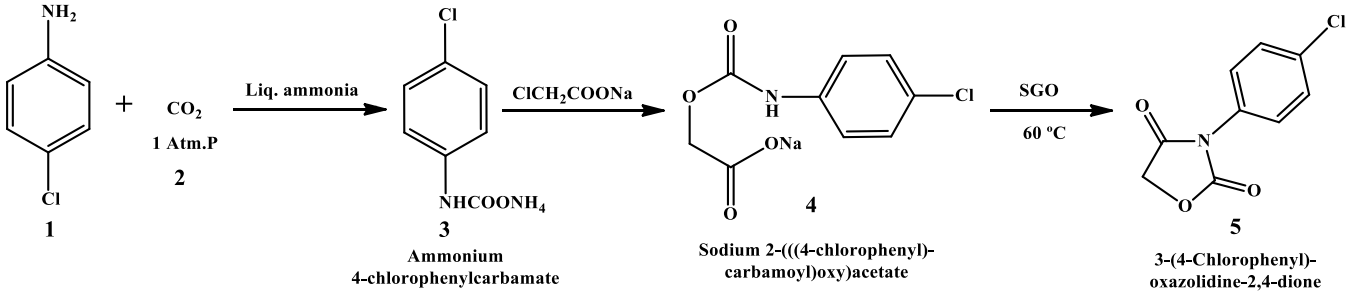

Scheme-I

TABLE-1
SGO CATALYZED CYCLIZATION FOR 3-(4-CHLOROPHENYL)OXAZOLIDINE-2,4-DIONE (**5**)

Entry	[a]Catalyst	Solvent	Temp. (ºC)	[b]Yield (%)
1	–	DMF	RT	0
2	HCl	DMF	RT	1-3
3	HCl	DMF	30	6
4	HCl	DMF	50	>6
5	TsOH	DMF	30	0
6	MsOH	DMF	30	>1-3
7	Graphite	DMF	30	>3
8	Graphene	DMF	30	>3
9	Graphite	DMF	45	>6
10	Graphene	DMF	45	>6
11	Graphene oxide	DMF	30	>11
12	Graphene oxide	DMF	45	>11
13	Graphene oxide	Toluene	30	>7
14	Graphene oxide	Toluene	45	>7
15	SGO (5 mg)	DMF	30	57
16	SGO (7.5mg)	DMF	45	89
17	SGO (10mg)	DMF	80	94
18	0	DMF	80	0
19	SGO (7.5mg)	DMF	80	75
20	SGO (5 mg)	DMF	80	40
21	SGO (7.5mg)	Toluene	45	87
22	SGO (10mg)	Toluene	80	90
23	SGO (5 mg)	CH_3CN	30	69
24	SGO (7.5mg)	CH_3CN	45	78
25	SGO (10mg)	CH_3CN	80	80

[a]A mixture of **6a** (1.00 mmol) and SGO (20 wt.%) in the solvent (10 mL) was stirred at the mentioned temperature.
[b]Isolated product yield.

completion the reaction, cool to room temperature and then poured the mixture onto crushed ice. The obtained precipitate was neutralized to pH ~7 with solid $NaHCO_3$, filtered, washed with cold water and finally dried to obtain hydrazone derivatives (**8a-h**).

Then, in a dry, nitrogen-flushed flask was charged with hydrazine derivatives **8a-h** and anhydrous THF followed by the addition of $POCl_3$ dropwise. After complete addition, the reaction was warmed to 80 ºC and refluxed for 5 h. The mixture was then cooled to room temperature and carefully poured onto crushed ice with vigorous stirring. The pH was adjusted to 9 using 10% aqueous Na_2CO_3 and the product was extracted with ethyl acetate. The crude product was purified by column chromatography (hexane/EtOAc 6:2) to afford the substituted pyrazole derivatives (**9a-h**) (**Scheme-II**).

Synthesis of pyrazole containing 1,3-oxazolidine-2,4-dione derivative (10) (step-6): In a dry 50 mL round-bottom flask fitted with a reflux condenser and nitrogen inlet, 3-(4-chlorophenyl)-1,3-oxazolidine-2,4-dione (**5**, 1.0 equiv., 1.0 mmol) was mixed with the substituted pyrazole derivative (**9a**) in the presence of fused sodium acetate (1.5 equiv.) and absolute ethanol (10 mL). The reaction mixture was stirred and refluxed at ~78 ºC for 6 h. Progress was monitored by TLC (hexane/EtOAc6:4); the disappearance of **5** (higher R_f, UV-active) and the appearance of a less mobile product indicated the completion of the reaction. After cooling to room temperature, the inorganic solids were filtered and washed with warm ethanol (2 × 10 mL). The filtrate was concentrated and the crude product was purified by flash column chromatography (hexane/EtOAc, 6:4) to yield the target heterocyclic compound **10a** as pale solid (**Scheme-III**). The same procedure was applied to synthesize other derivatives.

(*E*)-3-(4-Chlorophenyl)-5-((1-phenyl-3-(*p*-tolyl)-1*H*-pyrazol-4-yl)methylene)oxazolidine-2,4-dione (10a): Yield: 88%; white crystalline solid; m.p.: 192-194 ºC; HRMS (ES^+) calcd. for $C_{26}H_{18}ClN_3O_3$ $[M+H]^+$: 456.10; found: 456.09; IR (KBr, ν_{max}, cm^{-1}): 3100, 3030 (Ar-H *str*., pyrazole-H *str*.), 1716 (C-O *str*.), 1587, 1525, 1442 (C-N, C-C, aromatic ring),

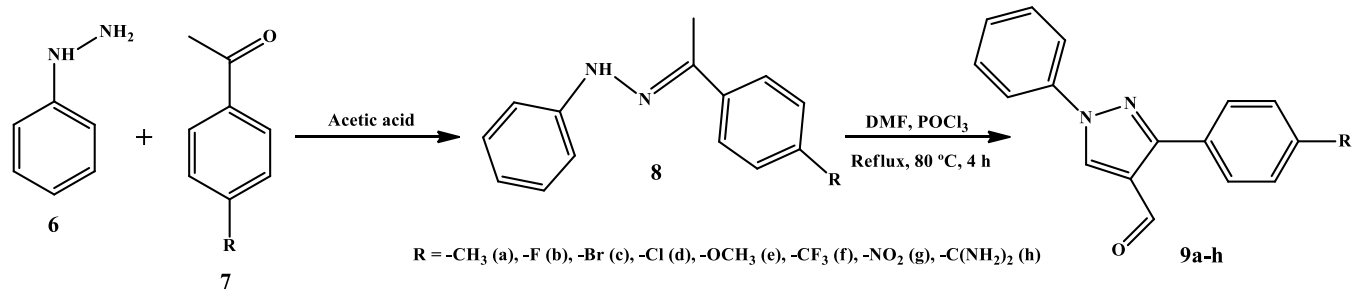

Scheme-II

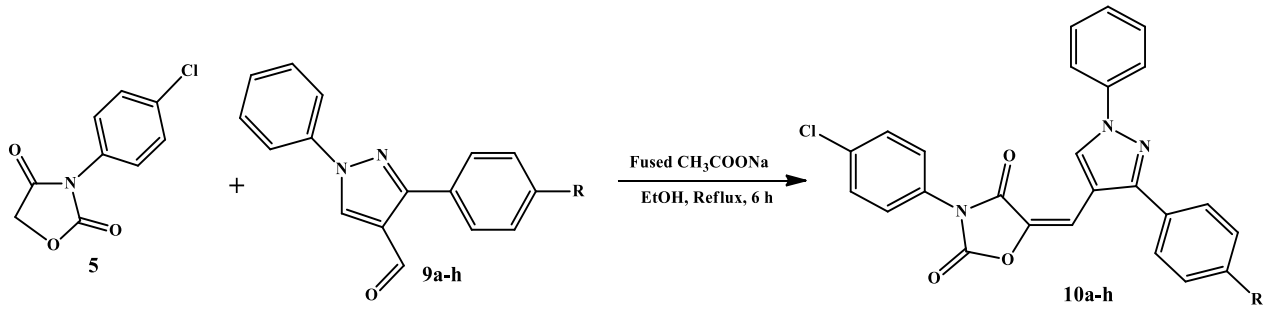

R = -CH_3 (a), -F (b), -Br (c), -Cl (d), -OCH_3 (e), -CF_3 (f), -NO_2 (g), -$C(NH_2)_2$ (h)

Scheme-III

1336 (C-S *str*.), 685 (C-S-C linkage); ^{1}H NMR (400 MHz, DMSO-d_6, δ ppm): 8.86 (s, 1H, C-CH group in pyrazole ring), 8.10-7.38 (m, 14H, Ar-H, C-NH, -C-CH), 6.31 (s, 1H, =CH), 2.31 (s, 3H, Ar-H); 192.4, 165.3, 163.8, 161.7, 152.8, 137.7, 134.1, 131.1, 130.6, 129.4, 128.9, 128.3, 127.4, 122.6, 122.0, 119.3, 116.2, 115.6.

(*E*)-3-(4-Chlorophenyl)-5-((3-(4-fluorophenyl)-1-phenyl-1*H*-pyrazol-4-yl)methylene)oxazolidine-2,4-dione (10b): Yield: 84%; white crystalline solid; m.p.: 198-201 ºC; HRMS (ES$^+$) calcd. for $C_{25}H_{15}ClFN_3O_3$ [M+H]$^+$: 460.08; found: 460.06; IR (KBr, ν_{max}, cm^{-1}): 3101, 3059 (Ar-H *str*., pyrazole-H *str*.), 1717 (C-O *str*.), 1590, 1520, 1443 (C-N, C-C, aromatic ring), 1340 (C-S str.), 680 (C-S-C linkage); ^{1}H NMR (400 MHz, DMSO-d_6, δ ppm): 8.72 (s, 1H, CH group in the pyrazole ring), 8.10-7.49 (m, 14H, Ar-H, C-NH, C-CH) 6.41 (s, 1H, =CH); ^{13}C NMR (400 MHz, DMSO-d_6, δ ppm): 193.6, 166.8, 153.5, 146.3, 139.3, 134.6, 131.2, 130.2, 130.0, 129.1, 128.0, 123.5, 122.0, 119.9, 116.0, 21.4.

(*E*)-5-((3-(4-Bromophenyl)-1-phenyl-1*H*-pyrazol-4-yl)methylene)-3-(4-chlorophenyl)oxazolidine-2,4-dione (10c): Yield: 86%; white crystalline solid; m.p.: 195-198 ºC; HRMS (ES$^+$) calcd. for $C_{25}H_{15}BrClN_3O_3$ [M+H]$^+$: 520.0; found: 520.03; IR (KBr, ν_{max}, cm^{-1}): 3119, 3063 (Ar-H *str*., pyrazole-H *str*.), 1716 (C-O *str*.), 1593, 1522, 1440 (C-N, C-C aromatic ring, 1340 (C-S *str*.), 680 (C-S-C linkage); ^{1}H NMR (400 MHz, DMSO-d_6, δ ppm): 8.76 (s, 1H, CH group in the pyrazole ring), 8.10-7.48 (m, 14H, Ar-H, C-NH, C-CH), 6.34 (s, 1H, =CH); ^{13}C NMR (400 MHz, DMSO-d_6, δ ppm): 192.8, 166.6, 152.4, 134.4, 130.2, 130.9, 130.5, 130.0, 129.70, 129.3, 129.1, 128.1, 123.2, 122.6, 120.1, 117.1.

(*E*)-3-(4-Chlorophenyl)-5-((3-(4-chlorophenyl)-1-phenyl-1*H*-pyrazol-4-yl)methylene)oxazolidine-2,4-dione (10d): Yield: 83%; white crystalline solid; m.p.: 195-197 ºC; HRMS (ES$^+$) calcd. for $C_{25}H_{15}Cl_2N_3O_3$ [M+H]$^+$: 476.05; found: 476.06; IR (KBr, ν_{max}, cm^{-1}): 3093, 3061 (Ar-H *str*., pyrazole-H *str*.), 1732 (C-O *str*.), 1592, 1493, 1432 (C-N, C-C aromatic ring), 1340 (C-S *str*.), 681 (C–S–C linkage); ^{1}H NMR (400 MHz, DMSO-d_6, δ ppm): 8.68 (s, 1H, CH group in the pyrazole ring), 8.10-7.48 (m, 14H, Ar-H, C-NH, C-CH), 6.34 (s, 1H, =CH); ^{13}C NMR (400 MHz, DMSO-d_6, δ ppm): 193.6, 180.7, 166.6, 151.9, 140.0, 133.6, 133.5, 131.5, 130.17, 129.8, 129.1, 128.9, 128.3, 127.2, 122.0, 119.0, 115.1;

(*E*)-3-(4-Chlorophenyl)-5-((3-(4-methoxyphenyl)-1-phenyl-1*H*-pyrazol-4-yl)methylene)oxazolidine-2,4-dione (10e): Yield: 88%; white crystalline solid; m.p.: 192-194 ºC; HRMS (ES$^+$) calcd. for $C_{26}H_{18}ClN_3O_4$ [M+H]$^+$: 472.1; found: 472.09; IR (KBr, ν_{max}, cm^{-1}): 3102, 3030 (Ar-H *str*., pyrazole-H *str*.), 1711 (C-O *str*.), 1580, 1521, 1440 (C-N, C-C aromatic ring), 1336 (C-S *str*.), 681 (C–S–C linkage); ^{1}H NMR (400 MHz, DMSO-d_6, δ ppm): 8.80 (s, 1H, CH group in the pyrazole ring), 8.10-7.17 (m, 14H, Ar-H, C-NH, C-CH), 6.34 (s, 1H, =CH), 3.88 (s, 3H, Ar-OCH_3); ^{13}C NMR (400 MHz, DMSO-d_6, δ ppm): 193.3, 167.3, 160.0, 153.7, 137.6, 135.2, 130.8, 131.0, 129.8, 129.4, 128.5, 127.6, 123.3, 121.5, 119.5, 115.5, 115.4, 55.4.

(*E*)-3-(4-Chlorophenyl)-5-((1-phenyl-3-(4-(trifluoromethyl)phenyl)-1*H*-pyrazol-4-yl)methylene) oxazolidine-2,4-dione (10f): Yield: 86%; white crystalline solid; m.p.: 193-195 ºC; HRMS (ES$^+$) calcd. for $C_{26}H_{15}ClF_3N_3O_3$ [M + H]$^+$: 510.08; found: 510.09; IR (KBr, ν_{max}, cm^{-1}): 3100, 3060 (Ar-H *str*., pyrazole-H *str*.), 1716 (C-O *str*.), 1594, 1523, 1440 (C-N, C-C, aromatic ring), 1341 (C-S *str*.), 683 (C-S-C linkage); ^{1}H NMR (400 MHz, DMSO-d_6, δ ppm): 8.88 (s, 1H, CH group in the pyrazole ring), 8.13-7.50 (m, 13H, Ar-H, C-NH, C-CH), 6.34 (s, 1H, =CH); ^{13}C NMR (400 MHz, DMSO-d_6, δ ppm): 193.5, 166.4, 163.7, 161.7, 152.8, 137.6, 133.1, 130.0, 129.7, 129.0, 129.3, 128.7, 127.7, 122.8, 122.2, 119.5, 116.2, 115.8.

(*E*)-3-(4-Chlorophenyl)-5-((1-phenyl-3-(4-(nitro)-1*H*-pyrazol-4-yl)methylene)oxazolidine-2,4-dione (10g): Yield: 92%; white crystalline solid; m.p.: 196-197 ºC; HRMS (ES$^+$) calcd. for $C_{25}H_{15}ClN_4O_5$ [M+H]$^+$: 487.07; found: 487.09; IR (KBr, ν_{max}, cm^{-1}): 3124, 3086 (Ar-H *str*., pyrazole-H *str*.), 1718 (C-O *str*.), 1599, 1531, 1444 (C-N, C-C, aromatic ring), 1343 (C-S *str*.), 682 (C-S-C linkage); ^{1}H NMR (400 MHz, DMSO-d_6, δ ppm): 8.80 (s, 1H, CH group in pyrazole ring), 8.33-7.41 (m, 14H, Ar-H, C-NH, -C-H), 6.34 (s, 1H, =CH); ^{13}C NMR (400 MHz, DMSO-d_6, δ ppm): 193.8, 166.6, 150.6, 148.0, 138.6, 134.7, 133.0, 131.8, 131.33, 129.4, 128.4, 127.5, 126.7, 123.5, 123.1, 122.7, 121.6, 121.5, 120.6, 116.5.

(*E*)-3-(4-Chlorophenyl)-5-((1-phenyl-3-(4-(*N*,*N*-dimethylamine)-1*H*-pyrazol-4-yl)methylene)oxazolidine-2,4-dione (10h): Yield: 89%; white crystalline solid; m.p.: 198-199 ºC; HRMS (ES$^+$) calcd. for $C_{27}H_{21}ClN_4O_3$ [M+H]$^+$: 485.13; found: 485.11; IR (KBr, ν_{max}, cm^{-1}): 3100, 3029 (Ar-H *str*., pyrazole-H *str*.), 1714 (C-O *str*.), 1583, 1522, 1440 (C-N, C-C aromatic ring), 1337 (C-S *str*.), 683 (C-S-C linkage); ^{1}H NMR (400 MHz, DMSO-d_6, δ ppm): 8.88 (s, 1H, C-CH group in pyrazole ring), 8.11-7.38 (m, 14H, Ar-H, C-NH, C-CH), 6.34 (s, 1H, =CH), 3.01 (s, 3H, Ar-N(CH_3); ^{13}C NMR (400 MHz, DMSO-d_6, δ ppm): 192.8, 167.9, 153.5, 145.3, 139.5, 134.6, 131.2, 129.9, 130.0, 128.3, 127.0, 123.5, 122.2, 118.9, 117.0, 21.3.

Antimicrobial activity: The antibacterial activities of the synthesized compounds (**10a-h**) were evaluated against *E. coli*, *P. aeruginosa*, *S. aureus* and *S. pyogenes* using a microtiter plate-based growth inhibition assay [17]. Overnight cultures of each bacterial strain were grown in Luria-Bertani (LB) broth and subsequently diluted to an OD_{600} of 01. Aliquots of 100 µL of this diluted suspension were added to microtiter plate wells containing 100 µL of LB medium supplemented with the test compounds at the two different studied concentrations. Prior to the addition of bacterial cells, the compound solutions were irradiated at 365 nm for 15 min where indicated, in order to evaluate their light-mediated antibacterial effects. The plates were then incubated at 37 ºC with orbital shaking and bacterial growth was monitored by measuring OD_{600} every 10-15 min for 12 h using a microplate reader. A brief 30 s shaking step was included before each measurement. For data normalization, the initial OD_{600} value (time zero) was subtracted from all subsequent readings.

RESULTS AND DISCUSSION

The target series (*E*)-5-((1-phenyl-3-(*p*-tolyl)-1*H*-pyrazol-4-yl)methylene)-3-(*p*-tolyl)oxazolidine-2,4-dione (**10a-h**) was synthesized using sulfonated graphene oxide as catalyst. In brief, compound **1** was first reacted with CO_2 (1 atm.) in liquid NH_3 to generate ammonium 4-chlorophenylcarbamate (**3**), which was O-carboxymethylated with sodium 2-chloroacetate to give sodium 2-[((4-chlorophenyl)carbamoyl)oxy]acetate (**4**). Subsequent SGO (GO-SO_3H) catalyzed intramolecular N-acylation and dehydration at 80 ºC efficiently provided 3-(4-chlorophenyl)-1,3-oxazolidine-2,4-dione (**5**), with water as by-product. In parallel, hydrazones (**8**) were synthesized by condensation of phenylhydrazine derivatives with 1-(4*R*-phenyl)-ethan-1-ones in acetic acid, followed by cyclization under Vilsmeier conditions to yield 1-phenyl-3-(*p*-tolyl)-1*H*-pyrazole-4-carbaldehydes (**9a-h**). Electron-withdrawing substituents enhanced the reaction rates and slightly improved yields relative to electron-donating groups (*e.g.* Me, OMe).

Coupling of compound **5** with pyrazole-4-carbaldehydes (**9a-h**) in ethanol under reflux with fused sodium acetate produced the target hybrids (**10a-h**) in good-to-excellent yields. The reaction proceeds *via* enolate formation at C-5 of compound **5**, nucleophilic addition to the aldehyde and acetate assisted dehydration. The structural characterization confirmed the formation of the conjugated products, for example, disappearance of the aldehyde C=O stretch and appearance of C=C in IR, loss of –CHO proton and emergence of vinylic =CH at δ ≈ 7.7-8.3 ppm in ^{1}H NMR, retention of imide-dione carbonyls (δ ≈ 173-182 ppm in ^{13}C NMR) and the $[M+H]^+$ in HRMS with isotopic patterns for Cl, F or NO_2. The exocyclic double bond was assigned *E*-geometry based on the vinylic shifts and sterically favoured anti-elimination. The optimized conditions (DMF solvent, 10 mg SGO/mmol) enabled completion of the cyclization and Knoevenagel steps within ~6 h, providing a short, metal-free route to diversely substituted pyrazole-oxazolidine hybrids.

Acidity and surface functional groups of SGO: Since SGO is a non-stoichiometric and heterogeneous material, the concentrations of acidic groups are expressed in mmol g^{-1}, rather than an exact number per sheet. The calculated acidic functional groups were carboxyl groups: 3.11 mmol g^{-1}, sulfonyl (SO_3H) groups: 7.89 mmol g^{-1} and phenolic groups: 2.33 mmol g^{-1}. The sulfonic acid content obtained from titration was consistent with the sulfur atomic percentage measured by EDX (8.0%), confirming successful sulfonation of the GO framework. Carboxyl group concentration was determined by subtracting the sulfonic contribution from the $NaHCO_3$ titration results, while phenolic acidity was obtained by subtracting both carboxyl and sulfonic groups from the Na_2CO_3 titration data. The high density of accessible acidic sites is responsible for the enhanced catalytic performance of SGO under optimized conditions (Table-1). Hence, SGO functions as an efficient metal-free nanocarbon catalyst for the synthesis of pyrazole-oxazolidine derivatives under mild reaction conditions.

Characterization of SGO: The morphological features of GO and SGO were verified by SEM and TEM analysis. The surface area of the SGO nanomaterial is roughly 1.5-5 µm × 7-8 µm. The wrinkled sheet-type shape was observed in SEM image (Fig. 1a), which further proposed that the microstructure of nanoGO layers are successfully conserved during the process of sulfonation [14,16]. It was observed that the restacking of graphene oxide layers through π–π interactions during the chemical modification process of sulfonation was accountable for the estimated thickness or width of the SGO nanomaterial sheet, which is around 1.8 nm (Fig. 1b). The EDS spectrum of sulfonated graphene oxide (SGO) displayed distinct peaks corresponding to C, O and S (Fig. 1c). Ele-

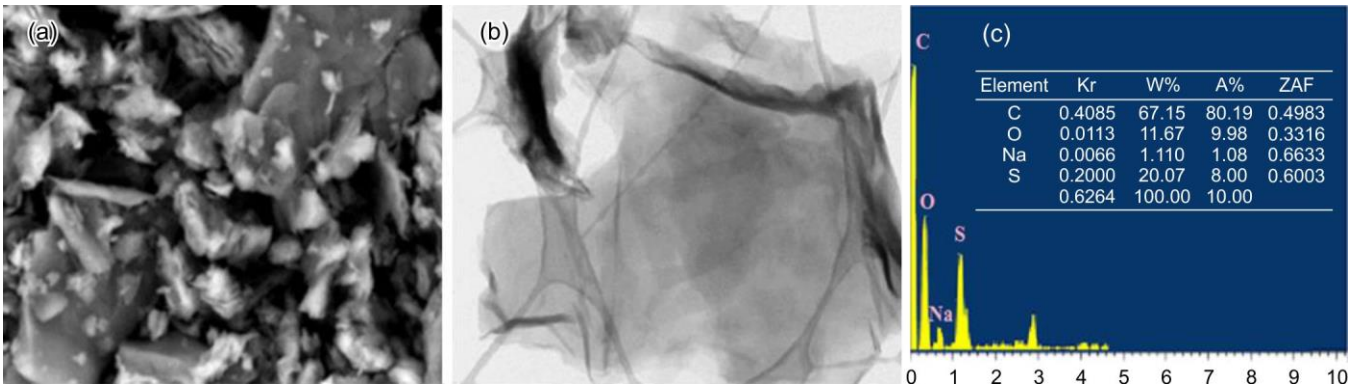

Fig. 1. SEM (a), TEM (b) and EDX (c) images of sulfonated graphene oxide (SGO) catalyst

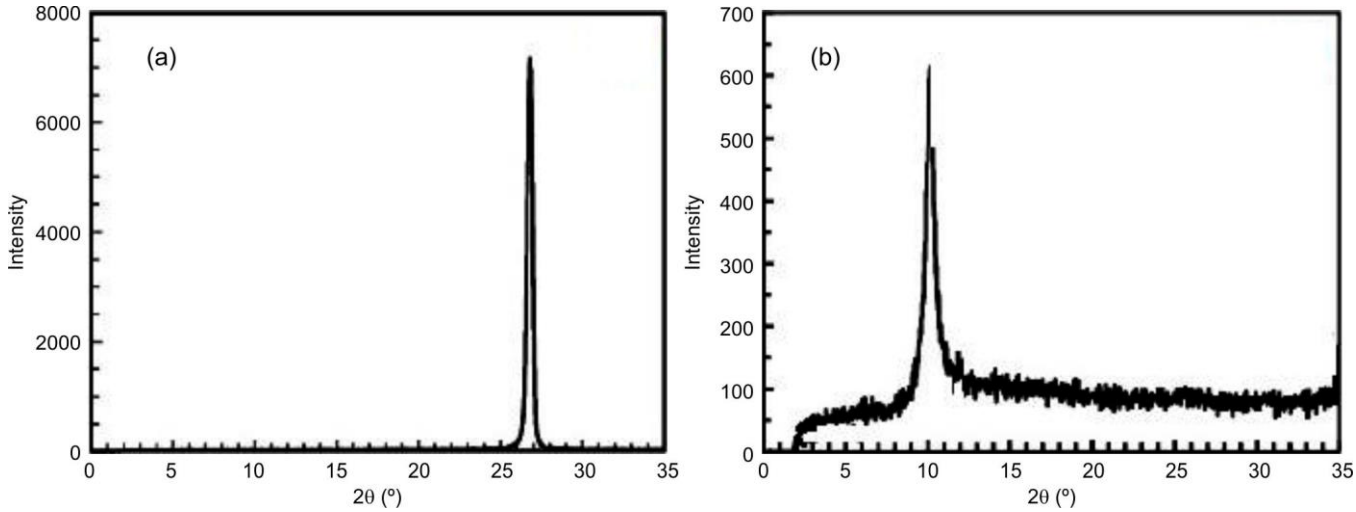

Fig. 2. XRD patterns of (a) GO and (b) SGO

mental analysis indicated that the synthesized SGO contained 20.07 wt.% sulfur, which is higher than values reported in previous studies [14,16]. From the atomic percentage data, the S/C ratio was calculated to be 0.10, confirming the successful functionalization of the graphene oxide surface with sulfonic acid groups

Fig. 2 illustrates the X-ray diffraction patterns of GO and SGO. The XRD pattern of pristine graphite oxide exhibited a characteristic diffraction peak at 2θ = 26.9º (Fig. 2a), corresponding to the (002) plane of the hexagonal graphite structure, with an interlayer spacing of 0.35 nm. In contrast, the SGO sample showed a diffraction peak at 2θ = 10.4º (Fig. 2b), corresponding to the (001) plane of the hexagonal crystal structure, with a *d*-spacing of 0.88 nm [16,18]. The increased interlayer distance indicates the introduction of hydroxyl and other oxygen containing functional groups into the carbon layers. The average number of nanolayers in SGO was determined to be 8, compared to 62 layers in pristine graphite.

Recycling of SGO nanocatalyst: The reusability of the SGO catalyst was further investigated to assess its stability and catalytic efficiency over multiple cycles. Under the optimized conditions, SGO was recycled and tested for four consecutive reactions. After completion of each reaction, the catalyst was recovered by filtration, washed with deionized water and methanol, and dried at 120 ºC for 1.5 h in a hot-air oven. The conversion for each cycle is illustrated in Fig. 3, demonstrating consistent catalytic activity and stability [18].

Antimicrobial activity: The antibacterial activities of the synthesized compounds (**10a-h**) were evaluated against *E. coli*, *P. aeruginosa*, *S. aureus* and *S. pyogenes* using the serial broth dilution method. Chloramphenicol served as the reference drug and the MIC values were determined based on complete inhibition of bacterial growth (99.99-100%). Among all the derivatives, compounds **10b**, **10d** and **10f** exhibited the highest antibacterial activity, showing the inhibition efficiency nearly similar to chloramphenicol at both 50 and 100 µg/mL (Table-2).

Moreover, compound **10c** showed slightly reduced activity compared to these highly active halogenated analogues but still maintained strong inhibition in the range of 98.80-99.00%.

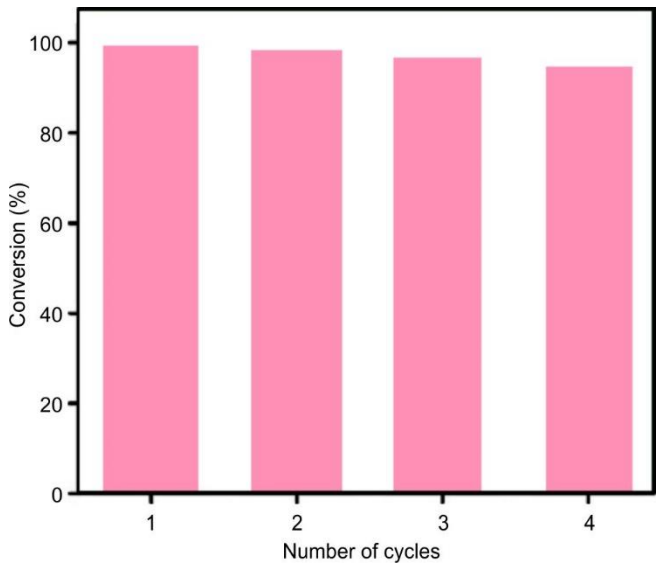

Fig. 3. Recycling performance data of the nanocatalyst SGO

The methyl-substituted compound **10a** showed markedly lower activity, indicating that electron-withdrawing halogens significantly enhance antibacterial potency, while electron-donating groups reduce it. Furthermore, compounds **10e** and **10g** demonstrated moderate inhibition (87-89%), whereas **10h** showed intermediate activity lower than the most active halogenated derivatives but higher than the weak-to-moderate performers. Overall, the results reveal a clear structure activity trend: halogen substitution enhances antibacterial efficacy, with compounds **10b**, **10d** and **10f** showing the strongest broad-spectrum activity comparable to the standard drug.

Conclusion

In this work, sulfonated graphene oxide (SGO) was successfully synthesized *via* the sulfonation of graphene oxide (GO) using a diazonium salt of sulfanilic acid under ultrasonic irradiation. The resulting SGO exhibited high surface area, strong acidic sites and excellent dispersibility, making it an effective nanocatalyst for the organic transformations.

TABLE-2
ANTIMICROBIAL ACTIVITIES DATA OF COMPOUNDS (**10b**, **10d**, **10f**)

Name of the bacteria	Compound **10b**		Compound **10d**		Compound **10f**	
	(50 µ/mL) inhibition rate (%)	(100 µ/mL) inhibition rate (%)	(50 µ/mL) inhibition rate (%)	(100 µ/mL) inhibition rate (%)	(50 µ/mL) inhibition rate (%)	(100 µ/mL) inhibition rate (%)
E. coli	99.20	99.90	99.10	99.40	99.40	99.99
S. aureus	99.50	99.90	99.30	99.70	99.90	100.00
S. pyogenes	99.40	99.94	99.30	99.90	99.60	99.99
P. aeruginosa	99.50	99.98	99.40	99.88	99.56	99.89
Bacterial culture (control)	100.00	100.00	100.00	100.00	100.00	100.00

*Chloramphenicol is a standard antibiotic drug for comparative study of the prepared samples against selected bacteria.
Observed antibacterial rate of Inhibitions (%) for the synthesized organic pyrazole-oxazolidine derivatives based small molecules.

Using SGO, 1,2-diacylhydrazines were efficiently cyclized to afford pyrazole-containing 1,3-oxazolidine-2,4-dione derivatives (**10a-h**). These compounds demonstrated remarkable antibacterial activity against both Gram-positive (*S. aureus*, *S. pyogenes*) and Gram-negative (*P. aeruginosa*, *E. coli*) bacterial strains, with inhibition zones approaching complete suppression (99.99-100%). This study highlights the potential of SGO as a versatile nanocatalyst for the synthesis of biologically active heterocycles and underscores the promising antimicrobial properties of the synthesized pyrazole containing 1,3-oxazolidine-2,4-dione derivatives.

CONFLICT OF INTEREST

The authors declare that there is no conflict of interests regarding the publication of this article.

DECLARATION OF AI-ASSISTED TECHNOLOGIES

During the preparation of this manuscript, the authors used an AI-assisted tool(s) to improve the language. The authors reviewed and edited the content and take full responsibility for the published work.

REFERENCES

1. I. Ameziane El Hassani, K. Rouzi, H. Assila, K. Karrouchi and M. Ansar, *Reactions*, **4**, 478 (2023); https://doi.org/10.3390/reactions4030029
2. B. Zeynizadeh, S. Rahmani and E. Eghbali, *Polyherdon*, **168**, 57 (2019); https://doi.org/10.1016/j.poly.2019.04.035
3. S. Ko and C.F. Yao, *Tetrahedron*, **62**, 7293 (2006); https://doi.org/10.1016/j.tet.2006.05.037
4. A.S. Kritchenkov, A.R. Egorov, A.A. Artemjev, I.S. Kritchenkov, O.V. Volkova, E.I. Kiprushkina, L.A. Zabodalova, E.P. Suchkova, N.Z. Yagafarov, A.G. Tskhovrebov, A.V. Kurliuk, T.V. Shakola and V.N. Khrustalev, *Int. J. Biol. Macromol.*, **149**, 682 (2020); https://doi.org/10.1016/j.ijbiomac.2019.12.277
5. L.M. Wang, J. Sheng, L. Zhang, J.-W. Han, Z.-Y. Fan, H. Tian and C.-T. Qian, *Tetrahedron*, **61**, 1539 (2005); https://doi.org/10.1016/j.tet.2004.11.079
6. S. Sheik Mansoor, K. Aswin, K. Logaiya and S.P.N. Sudhan, *J. Saudi Chem. Soc.*, **20**, S100; https://doi.org/10.1016/j.jscs.2012.09.010
7. A. Singh, V. Palakollu, A. Pandey, S. Kanvah and S. Sharma, *RSC Adv.*, **6**, 103455 (2016); https://doi.org/10.1039/C6RA22719H
8. S.S. Makone and D.B. Vyawahane, *Int. J. Chemtech Res.*, **5**, 1550 (2013).
9. H.R. Sonawane, J.V. Deore and P.N. Chavan, *ChemistrySelect*, **7**, e202103900 (2022); https://doi.org/10.1002/slct.202103900
10. M.V. Murali Krishna, J.C. Rao, S.S.K. Kothapalli, M. Brahmayya, K.C. Vineela, K.T.V. Rao, S. Marupati, M. Padma and S. Indla, *Discover Catal.*, **2**, 14 (2025); https://doi.org/10.1007/s44344-025-00018-3
11. D.G. Gil-Gavilán, J. Amaro-Gahete, R. Rojas-Luna, A. Benítez, R. Estevez, D. Esquivel, F.M. Bautista and F.J. Romero-Salguero, *ChemCatChem*, **16**, e202400251 (2024); https://doi.org/10.1002/cctc.202400251
12. M. Mirza-Aghayan, M.M. Tavana and R. Boukherroub, *Ultrason. Sonochem.*, **29**, 371 (2016); https://doi.org/10.1016/j.ultsonch.2015.10.009
13. Anjali, A. Mishra, M. Khurana, B. Pani and S.K. Awasthi, *ChemistrySelect*, **10**, e202404742 (2025); https://doi.org/10.1002/slct.202404742
14. M. Brahmayya, S.A. Dai and S.-Y. Suen, *Sci. Rep.*, **7**, 4675 (2017); https://doi.org/10.1038/s41598-017-04143-4
15. M. Mirza-Aghayan, M. Molaee Tavana and R. Boukherroub, *Ultrason. Sonochem.*, **29**, 371 (2016); https://doi.org/10.1016/j.ultsonch.2015.10.009
16. M.V.M. Krishna, J.C. Rao, S.S.K. Kothapalli, M. Brahmayya, K.C. Vineela, K.T.V. Rao, S. Marupati, M. Padma and S. Indla, *Discov. Catal.*, **2**, 14 (2025); https://doi.org/10.1007/s44344-025-00018-3
17. E. Peeters, H.J. Nelis and T. Coenye, *J. Microbiol. Methods*, **72**, 157 (2008); https://doi.org/10.1016/j.mimet.2007.11.010
18. M. Brahmayya, S.Y. Suen and S.A. Dai, *J. Taiwan Inst. Chem. Eng.*, **83**, 174 (2018); https://doi.org/10.1016/j.jtice.2017.12.003